IEEE Access
Multidisciplinary | Rapid Review | Open Access Journal

Received November 29, 2018, accepted December 23, 2018, date of publication January 8, 2019, date of current version January 29, 2019.

Digital Object Identifier 10.1109/ACCESS.2018.2890612

Damage Characteristics and Microstructure Response of Steel Alloy Q235B Subjected to Simulated Lightning Currents

YAKUN LIU[1], (Member, IEEE), MINGQIU DAI[1], ANIRBAN GUHA[2], XIN GAO[3], AND ZHENGCAI FU[1], (Member, IEEE)

[1]Department of Electrical Engineering, Shanghai Jiao Tong University, Shanghai 200030, China
[2]Department of Physics, Tripura University, Tripura 799022, India
[3]State Key Laboratory of Chemicals Safety, Sinopec Research Institute of Safety Engineering, Qingdao 266000, China

Corresponding author: Zhengcai Fu (zcfu@sjtu.edu.cn)

This work was supported by the National Key Research and Development Program of China under Grant 2017YFC1501506.

ABSTRACT This paper elucidates the damage characteristics, microstructure response and temperature rise of steel alloy Q235B suffered from lightning currents, which is the basis for lightning protection of oil tanks. Damage is inflicted in the designed Q235B specimens by using the multi-waveform multi-pulse impulse current generator to characterize the damage response induced by four typical lightning current components. The changes in the element composition and micro-hardness of Q235B are documented in the experiment. The microstructure changes in response to the temperature rise are analyzed by the proposed lightning-metal temperature rise model. The results reveal that, first, return stroke current with an amplitude of 201.2 kA leads to the largest damaged area of 3523.8 mm^2. Continuing current in the stroke intervals with a charge transfer of 12.1 C results in the damaged area of 12.6 mm^2 and the damaged depth of 0.5 mm. Long continuing current after stroke with a charge transfer of 210.1 C leads to the deepest damaged depth of 3.0 mm. The demixing phenomenon occurs on the cross-section, forming the damage zone, transition zone, and origin zone. The damage zone mainly consists of martensite transferred from pearlite and ferrite at temperature 990 °C. The transition zone is mainly martensite and ferrite forming at temperature 900 °C. The hardness of the three zones is 450, 310, and 180, respectively. The damaged depth is only 0.001 mm caused by the subsequent return stroke current with an amplitude of 102.2 kA.

INDEX TERMS Steel alloy, lightning currents, damage characteristics, temperature rise, microstructure response.

I. INTRODUCTION

Lightning protection of oil terminal is a controversial subject within two conflicting protection criteria of using self-protection criteria and installing lightning protection system (LPS) [1]. In China, the air terminal is not usually recommended in oil tank farms, making the metal structures themselves as standalone lightning interception points [2]. Although the metallic thickness, reliable bonding, and operational conditions are strictly fulfilled to reduce the lightning-induced risks, there still are more lightning-induced accidents than one could expect in the oil tank farms [3], [4]. The ignition threats and fire hazards in the non-LPS oil tank farms are mainly posed by the puncturing and hot-spot efforts at lightning attachments due to lack of air terminals for intercepting with lightning step leaders. It has been discovered that the discharge sparks with energy larger than 0.2 mJ could ignite the gas/air mixtures with gas volume fraction exceeding 1% [5]. The spontaneous combustion phenomenon of oil gas will occur when the hot-spot temperature reaches the self-ignition temperature, of which the temperature is 510∼530 °C for gasoline and 380∼425 °C for kerosene [3].

Steel alloy Q235B with robust mechanical characteristics and strong corrosion resistance is one kind of materials commonly used in the oil tanks [3]. Lightning can result in the damage on metal materials through thermal arc heating effects, resistive Joule effects, electric-magnetic force effects, and acoustic shock effects, which induce the

material splashing, melting or burning at the lightning attachments. Therefore, researching the interactions between steel alloy Q235B and lightning currents, especially investigating its damage characteristics and temperature rise, are of considerable importance for lightning protection of oil tanks.

The cloud-to-ground(CG) flash usually consists of 2∼20 multiple return strokes [6]–[10], in which the currents are qualified into four representative components, the first return stroke current(FRSC), continuing current in the stroke intervals(CCISI), subsequent return stroke current(SRSC), and long continuing current after stroke(LCCAS), in the standard of API-RP-545 formulated by American Petroleum Institute(API) and specifically recommended for lightning protection of aboveground storage tanks for flammable or combustible liquids [9]. The research of direct lightning effects on metal to date mainly focuses on the visually-inspected damage results, such as damaged depth and area. Kern *et al.* [11] discussed the melting effects caused by impulse currents and concluded the punched thickness of metal sheets. Chemartin *et al.* [12] investigated the damage results of an aluminum panel under a 100 kA arc and specified the thermal and mechanical efforts in the metal-lightning interactions. Metwally *et al.* [13] presented the experimental results of rear-face temperature rise for different kinds of metal struck by the long-duration lightning current. However, little literature addresses the internal damage microstructure changes of material response to lightning currents, which may reduce the mechanical strength and structural performance. Furthermore, there is no easy way to distinguish the separate contributions of the four lightning current components to damage characteristics in the natural lightning-induced cases. Therefore, independently characterizing the metal damage responses, especially the microstructure changes, are of particular interest to throw light on the damage characteristics and physical responses of the stricken metal materials to different typical lightning current components.

As a preliminary part of a broader study, this paper is concerned with the damage characteristics, microstructure response, and temperature rise of steel alloy Q235B subjected to four separate lightning current components. The high-resolution scanning electron microscope(SEM), energy dispersive spectrometer(EDS), and micro-hardness tester are adopted to investigate the damage morphology on the surface, microstructure on the cross-section, and thorough documentation of changes in element composition and micro-hardness, respectively. The simulated metal damage experiment under lightning currents is introduced in Section 2. In the following, Section 3 details the metal microstructure responses measured by the high-resolution SEM, EDS, and micro-hardness tester. The microstructure changes responding to the temperature rise of Q235B are discussed in Section 4, which is analyzed by the proposed lightning-metal temperature rise model. The conclusions of this paper are stated in Sections 5.

II. METAL DAMAGE EXPERIMENT OF LIGHTNING CURRENTS

The Multi-Waveform Multi-Pulse Impulse Current Generator (MWMP-ICG), developed by Shanghai Jiao Tong University [3], is used to generate the four typical simulated lightning current components of FRSC, CCISI, LCCAS, and SRSC. FRSC is an impulse current with waveform of 30/80 μs and amplitude of 201.2 kA. CCISI is a unidirectional rectangular waveform lasting 2.3 ms with amplitude of 5.9 kA. LCCAS is a unidirectional rectangular waveform with 520.0 ms duration and amplitude of 404.0 A. SRSC is an impulse current with waveform of 4/10 μs and amplitude of 102.2 kA. The four output simulated current waveforms could be referred in Figure 2 in our previous research [14], [15].

As the restrictor aperture installed on electrode head would absorb part of the arc energy and shockwave impacts for the indirect electrode, we adopt the special-made direct electrode to reduce electrode jet and achieve the severer damage results compared with using indirect electrode, whose material is made by a kind of tungsten-copper alloy(tungsten mass fraction 80%, copper mass fraction 19%, named as W80) and manufactured by the technics of copper-infiltrated tungsten skeleton method in a high-temperature atmosphere. The technics could make the copper powder uniformly distributed inside the tungsten skeleton and enhance the conductivity and anti-erosion capability of W80. The electrode is shaped into semi-ellipsoid with head curvature radius 3 mm and installed on an insulating clamping device. The insulating clamping device is made of two pieces of insulating woods, eight Ethoxyline fasteners, and one copper-made connection bridge with thickness of 5 mm and width of 50 mm, which is designed to prevent the coupons moving caused by the electromagnetic force and shockwave impact. The electrode and insulating clamping device are shown in Figure 1.

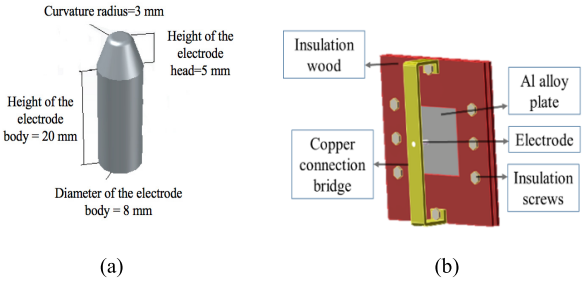

FIGURE 1. Experiment electrode and the designed fixture device (a) Electrode (b) Insulating clamping device.

The Q235B coupons are designed into the cuboid of size 150 mm(length) ×150 mm(width) ×5 mm(height) to meet the shape requirements of the following material inspections. These coupons are set up vertically to reduce the impacts of gravity. In order to stabilize the arc root, four symmetric grounding connections are installed with coupon contacting area more than 1500 mm^2 to conduct lightning currents

symmetrically to the ground. Arc root shows moveless characteristics when the discharge distance between the electrode and Q235B coupon is shorter than 10 mm [16]. And the metal damage volume decreases with discharge distance increasing. Therefore, the discharge distance is fixed at 5 mm in the experiment. The schematic diagram of the lightning metal damage experiment is illustrated in Figure 2.

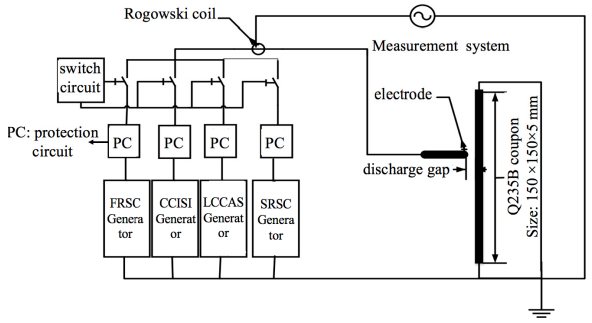

FIGURE 2. Schematic diagram of lightning metal damage experiment.

In order to decrease the influence of discharge dispersion, every experiment is carried out three times and the average results of the three tests are taken as the final results. We polish the Q235B coupons to wipe the oxidation layer on the surface, then clean and dry them step by step in every experiment. The damaged area and depth are measured by the ultrasonic B/C scanning system produced by the NDT Automation Inc. The high-speed infrared camera ThermaCAM^{TM} S65, with temperature measurement ranging up to 2000 °C and precision of 0.08 °C, is set up to measure the temperature rise of Q235B coupons struck by lightning. Experiment results of steel alloy Q235B under different lightning current components are presented in Table 1 and Figure 3.

TABLE 1. Experiment results of steel alloy Q235B under different lightning current components.

Lightning components	Amplitude /kA	Charge transfer /C	Damaged area/mm^2	Damaged depth/mm	Temperature rise/℃
FRSC	201.2	21.01	3523.80	0.01	597.5
CCISI	5.9	12.12	12.56	0.5	362.5
LCCAS	0.404	210.08	113.04	3.0	330.5*
SRSC	102.2	1.10	297.60	0.001	43.2

*Note that there is an extremely intense light emitting in the LCCAS experiment, which affects the temperature measurement on the front-face of metal. The rare-face temperature of Q235B coupons is measured by the high-speed infrared camera. The front-face temperature profile would be deduced by a numerical inversion model in Section IV.

From the damage results caused by the four lightning current components, it is concluded that the damaged area, damaged depth, and temperature rise show significant differences for the four components. The FRSC with current amplitude of 201.2 kA leads to the largest damaged area of 3523.8 mm^2, but with damaged depth only of 0.01 mm. The superficial damage morphology on the surface is dominated by the thin

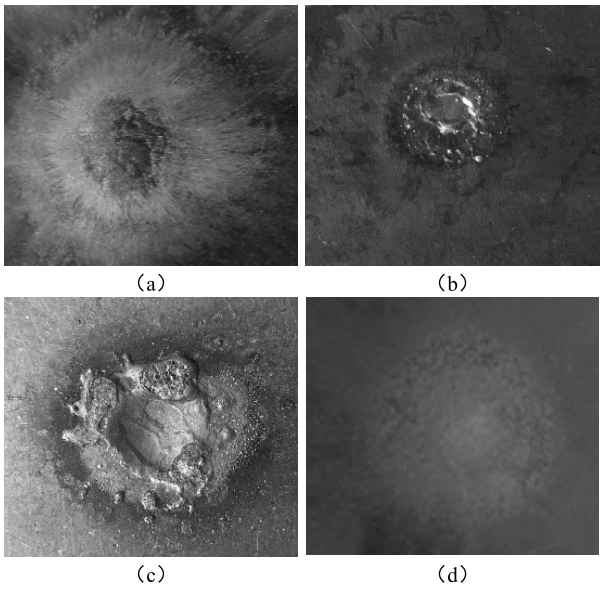

FIGURE 3. Damage characteristics of steel alloy Q235B under different lightning current components. (a) FRSC. (b) CCISI. (c) LCCAS. (d) SRSC.

layer spraying from the lightning attachment. The CCISI with charge transfer of 12.1 C results in the damaged area of 12.6 mm^2 and damaged depth of 0.5 mm for the Q235B coupon. The damage morphology on the surface is mainly the metal solidification after splashing. Suffered from the LCCAS with charge transfer of 210.1 C, the damaged depth increases obviously to 3.0 mm, meanwhile, the damaged area is 113.0 mm^2. The damage morphology on the surface are mainly pit, pores, and metal solidification after melting. A pit with diameter 5.6 mm is formed in the center of the damaged zone. Many pores appear at the rim of the pit. The damaged depth is only 0.001 mm subjected to the SRSC, while the damaged area is 297.6 mm^2. The damage morphology on the surface mainly consists of spots on the surface.

III. DAMAGE MICROSTRUCTURE OF Q235B UNDER LCCAS

A large flow of current and high velocity electric charge particles are injected into the metal within an extremely short time, which generate the Joule hear and arc energy to damage metal. The Joule heat can be calculated by the Equation 1. The arc energy generates the thermal stress on the Q235B through heat conduction and heat radiation, which can be calculated by the Equation 2.

$$Q_I = R \int i^2 dt \tag{1}$$

$$w = \int uidt = uQ \tag{2}$$

In Equation (1), R is the resistance of the metal. i is the current flowing through the metal. As Q235B is a kind of good conductor, the Joule heat is much smaller and can be neglected compared with the arc energy. In Equation (2), u is the arc voltage drop between the cathode and anode, which is 34.0 V measured in the experiment.

The LCCAS has the largest charge transfer of 210.1 C. Accordingly, the arc energy generated by LCCAS is the largest among the four lightning current components. The metal will undergo microstructure changes motivated by the elevated temperature within the current duration as long as 500 ms. Therefore, subsequent SEM testing is conducted to assess the microstructure of Q235B suffered from the LCCAS. The damage zone of the Q235B coupon is cut into two samples by a wire-cut machine and then cleaned three times with acetone, as shown in Figure 4. The Sample #1 is dried to prepare for observing the damage micro-morphology on the surface by the high-resolution SEM. The Sample #2 is inlayed with phenolic resin and then polished with waterproof abrasive paper from type 100#, 400#, 800#, 1500#, to 2000#. The polished coupons are dipped in the 4% Nital for 40 s and cleaned with acetone. After drying, the Sample #2 is observed to analyze the damage microstructure in cross-section by the high-resolution SEM JSM-7800 manufactured by Japan JEOL Ltd. The micro-hardness tester is measured by the ZHV30/zwickiLine hardness testing machine according to the Vickers hardness standard of EN ISO 6507.

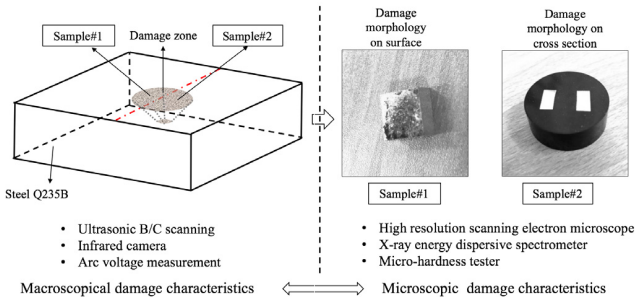

FIGURE 4. Sample processing flow chart.

The damage microstructure on the surface is shown in Figure 5. The cracks with width 10 μm and melting pits with diameter 50 μm$\sim$10 mm are observed on the surface. The lightning arc will not only lead to the macroscopical craters shown in Figure 3 but also result in many tiny melting pits displayed in Figure 5. The cracks are induced by the uneven thermal forces in the melting zone of metal. The melting pits are formed due to the vaporization and spatter of the melted metal.

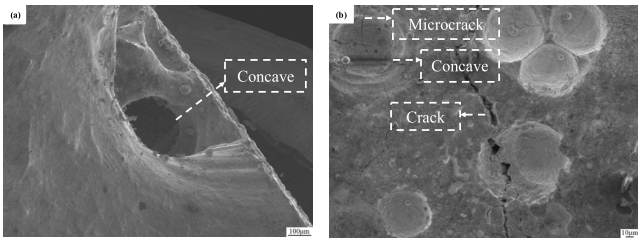

FIGURE 5. SEM images on the alloy Q235B sample's surface.

The damage microstructure in the cross-section is displayed in Figure 6, which can be divided into three zones,

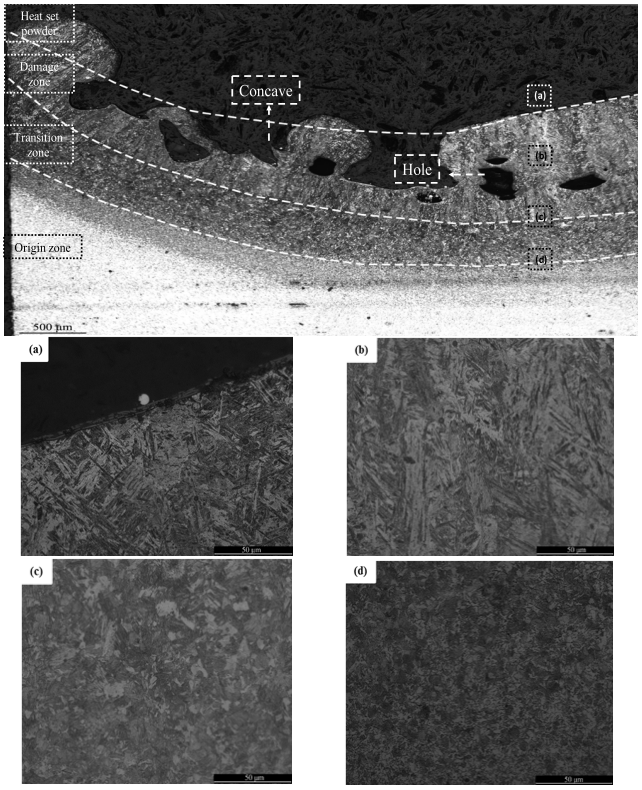

FIGURE 6. Damage microstructure on cross-section of Q235B.

the damage zone, transition zone, and origin zone. In the damage zone, the microstructure is dominated by Martensite (M), which is transferred from the Ferrite and Pearlite. Many cavities with diameter 150$\sim$500 μm are observed in this zone. Some featheriness Bainite (B) forms in the boundary between the damage zone and transition zone in the effects of the slow cooling rate. The transition zone mainly consists of the Martensite and Ferrite, which are formed between the critically-formed and fully-formed temperature of Austenite. Part of the Pearlite finishes the transformation to Martensite. The origin zone mainly consists of Ferrite and Pearlite. These grains are smaller and uniformly distributed in the origin zone.

Taking the typical part in the damage zone as an example, the contents of different elements are measured by using the EDS line scanning. The results are illustrated in Figure 7. Figure 7(a) shows that the content of oxygen element(O) increases along the EDS line scanning direction, reaching the maximum atom number 230 at the location of 45 μm, while the Fe element decreases meanwhile. It can be inferred that the oxygen layer with width 10 μm is formed in this area. Figure 7(b) indicates that the C and O elements increase in the crack area. The increase of C will prompt the material phase from γ to δ and result in the reduction of solubility for some elements, such as Si. The eduction of such elements will form some compound or Eutectic structure with lower melting point(900$\sim$1200 °C), of which the melting of

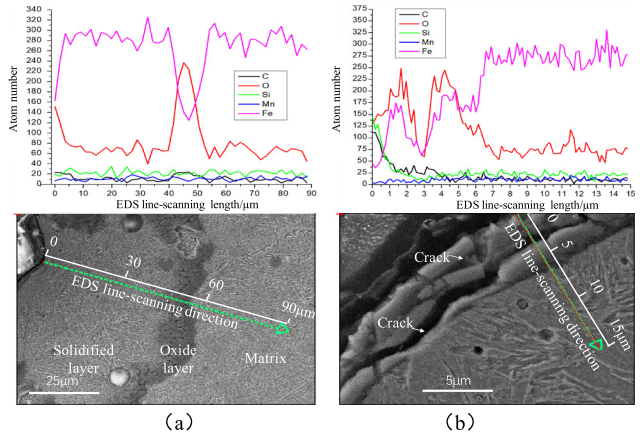

FIGURE 7. Element compositions on the surface of damage zone.

some low-melting materials will induce the tensile forces and shrinkage stresses. The tensile forces and shrinkage stresses will result in the cracks.

The average micro-hardness for the damage zone, transition zone, and origin zone are 450, 310, and 180 HV0.5, respectively, which are measured with 0.18 mm intervals and starting at the point 0.084 mm away from the coupon surface, as illustrated in Figure 8. The load of the probe is 0.5 kgf with duration 15.5 s setting in the ZHV30/zwickiLine hardness testing machine. It is concluded that the average micro-hardness of damage zone increases by 150 % compared with the origin zone. There exists an obvious gradient in the transition zone, of which the range could reach 250 HV0.5. This is because the micro-hardness of Martensite, Bainite, Pearlite, and Ferrite decreases in turn. The content of Martensite in damage zone is the highest and decreases along the three zones. Some Bainite appears in the interface of the damage zone and transition zone. Then the contents of Martensite decreases sharply, leading to the big gradient of micro-hardness in the transition zone.

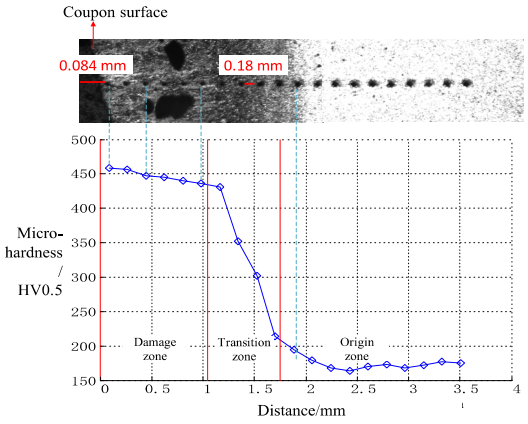

FIGURE 8. Micro-hardness value along sample damaged depth.

IV. MICROSTRUCTURE AND TEMPERATURE RISE ANALYSES

In the existing literature, most of the numerical approaches for calculating the material's thermal response to lightning and analyzing the electric-thermal coupling effects are based on a certain equation of describing the overall density variation rate, for instance, the Arrhenius equation is used for expressing the overall density variation rate of composite material [17]. Some core parameters in the corresponding equations are usually obtained from the thermogravimetric analysis(TGA) tests. However, the heating rate applied to the TGA tests(50 °C/min) is ten magnitudes lower than the rate under the lightning arc($\sim 10^{10}$ °C/min), which limits the accuracy of the numerical approaches. Therefore, another new lightning metal temperature model(LMTM) is proposed in the literature, in which the temperature distribution is inversely deduced based on the measured rear-face temperature rise data in the simulated lightning experiment and the heat conduction characteristics of metal material [18]. The heating rate of metal can reach $\sim 10^{10}$ °C/min in the proposed model, as it is acquired in the simulated lightning experiment.

According to the symmetry of the temperature rise, the temperature rises in one-fourth part of the Q235B coupon in 2-dimensions over time is calculated by LMTM and illustrated in Figure 9. The boiling point and melting point of Q235B are marked with the dashed line in Figure 9. The temperature on the rare-face of metal subjected to LCCAS with amplitude 404 A and charge transfer of 210.1 C will reach the highest at $t = 600$ ms according to the calculation results. When the node's temperature rise exceeds the melting point, the metal material will melt and form the pit. From the temperature profile and the position of the damaged nodes(nodes with the temperature higher than 1525 °C), the damaged depth suffered from LCCAS is 2.9 mm calculated by LMTM. The error is 3.3% compared with the experimental damaged depth of 3.0 mm.

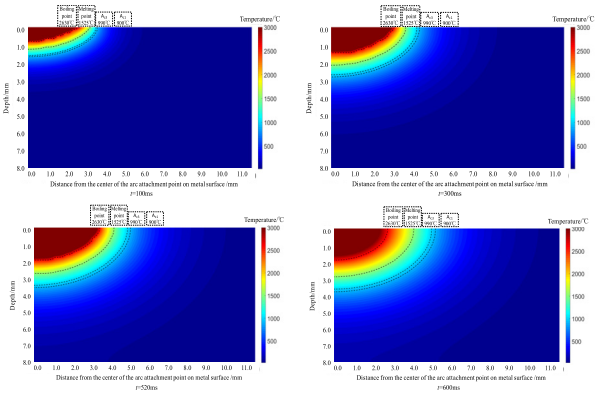

FIGURE 9. Temperature rise of the Q235B over time from $t = 100$ ms to $t = 600$ ms.

In Figure 9 and Figure 10, A_{c1} is the critical temperature of 900 °C for the Pearlite and Ferrite starting to transform into the Austenite. A_{c3} is the critical temperature of 990 °C

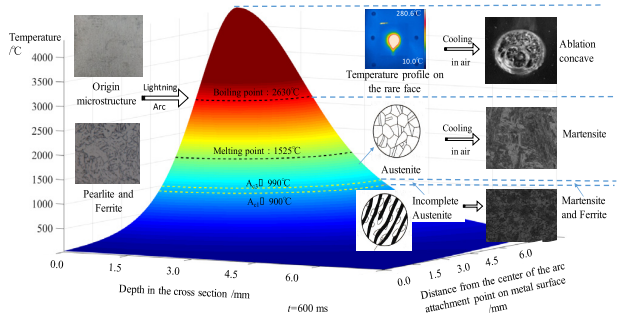

FIGURE 10. **Corresponding analyses between metal temperature profile in cross-section and microstructure.**

for the Pearlite and Ferrite finishing the transformation to the Austenite. The width between the temperature 900 °C and 990 °C is 0.1 mm at $t = 600$ ms as illustrated in Figure 10, which matches the microstructure observation results in Figure 6.

V. CONCLUSION

Steel alloy Q235B experiences significant microstructure changes, rapid temperature rise, and serious damage results exposed to the four typical lightning currents. The damage morphology on the surface, microstructure on the cross-section, element composition and micro-hardness changes are depicted using the simulated lightning experiment together with the proposed lightning-metal temperature rise model. The results show that,

(1) For the four lightning current components, the first return stroke current with amplitude of 201.2 kA results in the largest damaged area of 3523.8 mm^2. The damage morphology on the surface is dominated by the thin layer spraying from the lightning attachment. Caused by the continuing current in the stroke intervals with charge transfer of 12.1 C, the damaged area is 12.6 mm^2 and damaged depth is 0.5 mm. The long continuing current after stroke with charge transfer of 210.1 C leads to the deepest damaged depth of 3.0 mm, meanwhile the damaged area is 113.0 mm^2. The damage morphology on the surface are mainly pit, pores, and metal solidification after melting. Suffered from the subsequent return stroke current with amplitude of 102.2 kA, the damaged depth is only 0.001 mm.

(2) Suffered from the long continuing current after stroke, the demixing phenomenon occurs on the cross-section of Q235B, forming the damage zone, transition zone, and origin zone. The damage zone mainly consists of Martensite transferred from Pearlite and Ferrite at temperature 990 °C. The average micro-hardness of damage zone increases by 150 % compared with the micro-hardness of 180 in the origin zone. The transition zone is mainly Martensite and Ferrite with formation temperature of 900 °C, of which the average micro-hardness is 310.

(3) The damaged depth subjected to the long continuing current after stroke is 2.9 mm calculated by the lightning metal temperature model. The error is 3.3% compared with the experimental result of 3.0 mm. The width between the critically-formed temperature 900 °C and fully-formed temperature 990 °C is 0.1 mm at $t = 600$ ms, which matches the microstructure observation result of Pearlite, Ferrite, Austenite, and Martensite.

ACKNOWLEDGMENT

One of them would like to thank Earle Williams (Massachusetts Institute of Technology), Huizhong Jiang (Shanghai Jiao Tong University), and Dongyang Yang (Shanghai Jiao Tong University) for their support in this research.

REFERENCES

[1] D. A. Galván and C. Gomes, "Protection of oil storage tanks against direct lightning strikes: Self protection scheme or standalone LPS?" presented at the IEEE Int. Symp. Lightning Protection, 2014. [Online]. Available: https://www.infona.pl/resource/bwmeta1.element.ieee-art-000006729184

[2] X. Ren, Z. Fu, N. Yan, and W. Sun, "Analysis and experimental investigation of direct lightning protection for floating roof oil tanks," *Electr. Power Syst. Res.*, vol. 94, pp. 134–139, Jan. 2013, doi: 10.1016/j.epsr.2012.05.009.

[3] Y. K. Liu, X. Hailiang, and H. Yuwei, "Ablation damage and temperature rise of metal oil tanks struck by direct lightning," *High Voltage Eng.*, vol. 42, no. 5, pp. 1578–1585, May 2016, doi: 10.13336/j.1003-6520.hve.20160412028.

[4] E. Renni, E. Krausmann, and V. Cozzani, "Industrial accidents triggered by lightning," *J. Hazardous Mater.*, vol. 184, nos. 1–3, pp. 42–48, Dec. 2010, doi: 10.1016/j.jhazmat.2010.07.118.

[5] G. Hong, L. Quanzhen, S. Xiansheng, L. Xuqing, and L. Jianxiang, "Analysis of fire accidents caused by lightning strike on the seal ring of large floating roof tanks," *Saf. Health, Environ.*, vol. 8, no. 10, pp. 7–8, 2018.

[6] IEC Standard 62305, 2010, "Protection Against Lightning."

[7] SAE ARP Standard 5416, 2013, "Aircraft Lightning Test Methods."

[8] *Lightning Qualification Test Techniques for Aerospace Vehicles and Hardware*, Standard MIL-STD-1757A, 1980.

[9] *Recommended Practice for Lightning Protection of Above Ground Storage Tanks for Flammable or Combustible Liquids*, Standard API-RP-545, 2009.

[10] *Aircraft Lightning Environment and Related Test Waveforms*, Standard EUROCAE ED-84, 1997.

[11] A. Kern and W. J. Zischank, "Melting effects on metal sheets and air termination wires caused by direct lightning strikes," *Appl. Catal. A, Gen.*, vol. 401, nos. 1–2, pp. 20–28, 1988.

[12] L. Chemartin *et al.*, "Direct effects of lightning on aircraft structure: Analysis of the thermal, electrical and mechanical constraints," *AerospaceLab*, vol. 12, no. 5, pp. 1–15, 2012.

[13] I. A. Metwally, F. Heidler, and W. Zischank, "Measurement of the rear-face temperature of metals struck by lightning long-duration currents," *Int. Trans. Electr. Energy Syst.*, vol. 14, no. 4, pp. 201–222, Jul. 2013, doi: 10.1002/etep.16.

[14] Y. Liu, Z. Fu, X. Gao, T. Li, and M. Dai, "Damage characteristics and response of Al alloy 3003 to different components of simulated lightning currents," *IEEE Access*, vol. 6, pp. 1277–1283, 2017, doi: 10.1109/ACCESS.2017.2778197.

[15] Y. Liu, Z. Fu, Q. Liu, B. Liu, and A. Guha, "Experimental and analytical investigation on metal damage suffered from simulated lightning currents," *Plasma Sci. Technol.*, vol. 19, no. 12, pp. 37–45, Oct. 2018, doi: 10.1088/2058-6272/aa8aca.

[16] F. Uhlig, P. Gondot, B. Lepetit, J. Chabrerie, and P. Testé, "Experimental simulations of lightning impacts on aeronautical structural materials," presented at the Int. Aerosp. Ground Conf. Lightning Static Electr., 1995.

[17] Y. Wang, "Multiphysics analysis of lightning strike damage in laminated carbon/glass fiber reinforced polymer matrix composite materials: A review of problem formulation and computational modeling," *Comaposites A, Appl. Sci. Manuf.*, vol. 101, pp. 543–553, Oct. 2017.

[18] Y. Liu, Z. Fu, Q. Liu, B. Liu, and H. Xia, "Numerical inversion analysis on front-face temperature rise of Al alloy suffered from long continuing current in lightning," *IET Sci., Meas. Technol.*, vol. 12, no. 4, pp. 467–471, Jul. 2018, doi: 10.1049/iet-smt.2017.0222.

YAKUN LIU (M'13–D'18) received the B.S. degree in electric engineering from Xi'an Jiao Tong University, and the Ph.D. degree from Shanghai Jiao Tong University, China, in 2018, where he is currently with the Department of Electric Engineering. His current research interests include the lightning effects and lightning protection.

MINGQIU DAI (M'14) received the B.S. degree in electric engineering from Sichuan University, China, in 2013. She is currently pursuing the Ph.D. degree in electric engineering with Shanghai Jiao Tong University, China. Her current research interests include lightning protection measures for oil tanks and buildings.

ANIRBAN GUHA is currently a Senior Assistant Professor with the Department of Physics, Tripura University, India. His current research interests include lightning physics, global electric circuit, and ELF-VLF propagation inside the Earth-ionosphere waveguide.

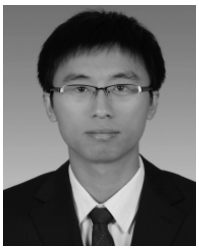

XIN GAO received the bachelor's degree in electronic information engineering from the Beijing University of Posts and Telecommunications, Beijing, China, in 2005, and the M.Eng. degree in electrical engineering from Shanghai Jiao Tong University, Shanghai, China, in 2011. He is currently a Senior Engineer with the Sinopec Research Institute of Safety Engineering, where he is involved in the electrical safety research. His current research interests include lightning safety, electrostatic safety, and electric explosion protection. His awards and honors include the Sinopec's Science and Technology Progress Award and the Chinese Academy of occupational Safety and Health Science and Technology Progress Award.

ZHENGCAI FU received the B.S., M.S., and Ph.D. degrees from Shanghai Jiao Tong University, China. From 1996 to 1998, he was a Research Assistant with The Hong Kong Polytechnic University. He is currently a Professor with Shanghai Jiao Tong University. He has authored three books, more than 200 articles, and more than 50 inventions. His current research interests include the direct lightning effects and lightning protection methodology for power systems, renewable energy systems, buildings, electronic systems and railway systems, lightning location, prediction, and warning technologies.